

Physics

Synthesis and characterization of nanofibers and nanocrystals of cellulose from *Guadua weberbaueri*

Síntese e caracterização de nanofibras e nanocristais de celulose de *Guadua weberbaueri*

Tiago Henrique da Costa Viana¹, Antonia Eliane Costa Sena¹, Maurício da Silva Souza¹,
Bruno Roseno de Souza Maia¹, Yuri Sotero Bomfim Fraga¹, Marcelo Ramon da Silva Nunes¹,
José Roberto de Lima Murad¹, Anselmo Fortunato Ruiz Rodriguez¹

¹Federal University of Acre, Rio Branco, Acre, Brazil

¹Federal Institute of Acre, Rio Branco, Acre, Brazil

ABSTRACT

The species *Guadua weberbaueri*, popularly known as bamboo or taboca and abundantly located in the region of Acre, Brazil, had its potential application as reinforcement to cementitious composites in civil construction explored through characterizations. For this purpose, preliminary steps were carried out, culminating in the preparation of cellulose nanofibers obtained from the bamboo pseudostem through various processes such as milling, sieving, pre-treatment, bleaching, elimination of hemicellulose and lignin to obtain cellulose, and acid hydrolysis of cellulose to obtain crystalline cellulose nanofibers (NCC). The NCC was characterized by infrared spectroscopy, thermogravimetric and thermal differential analyses, X-ray diffraction, X-ray fluorescence, dynamic light scattering, and fiber and cellulose contents. The results indicated predominantly crystalline nanomaterials with thermal stability up to 300 °C, carbonaceous bonds, and an abundance of sodium oxides and silica, indicating potential for incorporation into cementitious composites. This perspective, to be studied in later stages by the authors, aims to bring the fields of sustainability, civil construction, and nanotechnology closer together.

Keywords: *Guadua weberbaueri*; Cellulose nanofibers and nanocrystals; Structural reinforcement; Sustainability; Amazon

RESUMO

A espécie *Guadua weberbaueri*, popularmente conhecida como bambu ou taboca e encontrada em abundância na região de Acre, Brasil, teve seu potencial de aplicação como reforço em compósitos cimentícios na construção civil explorado por meio de caracterizações. Para isso, foram realizadas etapas preliminares, culminando no preparo de nanofibras de celulose a partir do pseudocaule do bambu por meio de diversos

processos, como moagem, peneiramento, pré-tratamento, branqueamento e eliminação de hemicelulose e lignina para obter celulose, seguido de hidrólise ácida da celulose para obter nanofibras de celulose cristalina (NCC). As NCC foram caracterizadas por espectroscopia infravermelha, análises termogravimétricas e diferencial térmico, difração de raios X, fluorescência de raios X, espalhamento dinâmico de luz e teores de fibras e celulose. Os resultados indicaram materiais nanoestruturados predominantemente cristalinos, com estabilidade térmica de até 300 °C, com ligações carbonáceas e uma abundância de óxidos de sódio e sílica, sugerindo um potencial de incorporação em compósitos cimentícios. Esta perspectiva, a ser explorada em estágios posteriores pelos autores, visa estreitar ainda mais os campos de sustentabilidade, construção civil e nanotecnologia.

Palavras-chave: *Guadua weberbaueri*; Nanofibras e nanocristais de celulose; Reforço estrutural; Sustentabilidade; Amazônia

1 INTRODUCTION

During the last decade, new nanofiber nanomaterials have been developed to be applied in civil construction in the form of bamboo nanofibers applying nanotechnology (Goetz et al., 2022; Miranda et al., 2022). In the structural area, species such as *Pinus taeda*, *Cereus jamacaru* and *Bambusa vulgaris* have been combined in cement matrices to improve hydration processes during curing, contributing to the development of new materials (Miranda et al., 2022).

At the intersection between civil construction and nanotechnology, in coherence with sustainability, there is the incorporation of nanomaterials in structural matrices, with a tendency towards cement (Barbosa et al., 2019; Campos et al., 2022; Lima et al., 2022; Mendes et al., 2022). Açai particles and fibers (*Euterpe oleracea* and *Euterpe precatoria*) indicated stabilities on the reinforcement base in the composition of reinforced composite products (Barbosa et al., 2019). MDF panels produced from *Eucalyptus grandis* particulate, incorporated into zinc oxide nanoparticles, improved mechanical resistance indices, demonstrating stability in physical properties (Campos et al., 2022). Wood with plastic characteristics, developed with *Astrocaryum murumuru* Mart., showed consistency in the physical and mechanical correlates (Lima et al., 2022). The nanocellulose used through cementitious composites, reflected effects on the mechanical performance, produced in trace control (Mendes et al., 2022).

Alongside the increasing use of cellulose-based composites, lignin levels are within desirable margins (Rambo et al., 2015; Jesus et al., 2019; Sasamori et al., 2022). To control and verification of the indices of compounds such as lignin, hemicellulose and cellulose itself, thermogravimetric analyzes seek to analyze plant biomass (from grass, coffee, banana stalks and açaí) and their degradation indices correlated to lignocellulosic compounds (Rambo et al., 2015). Using expandable polystyrene based on sugarcane bagasse, thermogravimetric and differential thermogravimetric analyzes identified points of stability and degradation (Jesus et al., 2019). In the case of polyethylene polymer, the thermal analysis, obtained from *Pinus Elliotti* wood, showed a high presence of lignin, to be applied in packaging and by-products (Sasamori et al., 2022).

In the aforementioned studies, materials of plant origin have potential application in civil construction (Morais, 2021; Alvarenga et al., 2022; Pescarolo et al., 2022). Gypsum composites, incorporated into *Bambusa tuldoides* fibers, obtained favorable mechanical performance (Alvarenga et al., 2022). The species *Guadua spp.* obtained mechanical potential for incorporation into the cementitious composite, in the form of nanofibers, provided improvement in the mechanical resistance indexes to traction and compression (Morais, 2021). Microfibers are also added to mortars, generating microfibrinous composites (Pescarolo et al., 2022).

In view of the above, the study proposes, as a factor of novelty and relevance, the synthesis of nanofibers and nanocrystals from a species of bamboo native and abundant in the state of Acre (Amazônia/Brazil), with potential that is still little known, for the civil construction industry.

The objective of the present study is to prepare and characterize *the Guadua weberbaeuri* cellulose nanofibers and nanocrystals in chemical and thermal form, aiming at their potential application as reinforcement to cementitious composites.

2 MATERIAL AND METHODS

2.1 Preliminary Steps

The collection of bamboo sticks and culms took place in the locations of the Federal University of Acre, Parque Zoobotânico (Figure 1), under the coordinates 9°57'25.0"S 67°52'12.6"W, where about 6 sticks were collected, with an average length of 3 m, and variable diameter.

The characterization of the species was based on the formulation of a exsiccate, under the tipping identification number N° UFACPZ 28061, containing bamboo leaf and stem (Figure 2), tipped in the Herbarium of the Universidade Federal do Acre, in the Parque Zoobotânico of Campus Rio Branco (Pereira, 2012).

Figure 1 – Geographical coordinates of the *Guadua weberbaeuri* bamboo sticks collection site



Source: Google Maps (2023)

Legend: Geographical coordinates of the *Guadua weberbaueri* bamboo sticks collection site, at Parque Zoobotânico, Universidade Federal do Acre

Figure 3 – (a) Bamboo cut for grinding; (b) ground bamboo



Source: Authors' private collection (October, 2022)

Legend: (a) Bamboo washed and cut into smaller dimensions for shredding poster; (b) bamboo crushed into powder

2.2 Sample production and chemical treatments

After drying, the culms obtained were taken to the knife mill, where they were ground and constituted the crushed bamboo sample (BT sample) (Arrais et al., 2016). After being ground, the pulp production process began, through delignification and bleaching (Correia, 2011; Cordeiro et al., 2014; Pego, Bianchi, & Veiga, 2019; Morais, 2021).

For delignification, the method was performed with a 2% NaOH solution, in the distribution proportion of 10 g of bamboo for 400 mL of solution, for 4 h at 80 °C and constant agitation, for 4 repetitions (Machado et al., 2014; Morais, 2021; Nunes et al., 2021). At the end of each repetition, the sample was washed with distilled water in large quantities, in sieves with an opening of 105 μm . From this step, the delignified cellulose pulp sample (PDC sample) originates.

In sequence, bleaching was performed using 24% (v/v) H₂O₂, as well as 4% (w/m) NaOH (1:1), following the distribution ratio of 1 g of fiber to 20 mL of solution

for 2 h at 50 °C temperature and constant stirring (Cordeiro et al., 2014; Morais, 2021). At the end of each repetition, the sample was washed with distilled water in large quantities, in sieves with an opening of 105 µm. From this step, the bleached cellulose pulp sample (PBC sample) originates.

Acid hydrolysis was performed with the samples. Prepared in a 64% H₂SO₄ solution, in the proportion of 1 g of pulp, 8.00 mL of acid and 8.00 mL of distilled water, with mechanical stirring at 45 °C for 35 minutes. At the end of hydrolysis, a ratio of 1 g of pulp to 20 mL of distilled water at 5 °C was used to neutralize the reaction (Samir, Alloin, & Dusfrene, 2005; Rosa et al., 2010).

Figure 4 – PDC samples (light brown coloring); PBC (white coloring) and NCC (dark brown coloring)



Source: Authors' private collection (October, 2022)

Legenda: PDC sample in light brown coloring; PBC sample in white coloring; NCC sample in dark brown coloring. The PDC and PBC samples are in the form of larger granules and the NCC sample is in powder form

2.3 Analyzes

2.3.1 Distribution of particle diameters

With the pulp, dynamic light scattering (DLS) analysis was initially performed to determine particle diameters, through intensity and volume of the sample. The reading occurred through the dilution of the samples, in a proportion of 0.005 g of sample for 1 mL of distilled water, then submitting the aqueous solution to the device's reading (Silvestro et al., 2023). The equipment is from the Malvern brand, with zetasizer nano specification - ZS90.

2.3.2 Crystallization of samples

X-ray Diffraction (XRD) measurements were performed using a diffractometer equipment, with voltage of 30 kV, analysis range between 3 and 80°, using copper filament, using an X-ray diffractometer BRUKER (model D2 PHASER, Cu-K α radiation), and reading degree of 2°/min, in continuous reading mode (Bilcati, Costa, & Paulino, 2022). For the SHIMADZU program (Pmgr) was used to determine the phases present with the JCPDS database. Sample preparation was performed using the powder method pressed randomly into the sample holder.

2.3.3 Fiber and cellulose content

Once the pulp is obtained, for chemical characterization, it is necessary to divide the cellular compound from the cell wall. The method used was the NDF/ADF, based on neutral detergent and acid detergent (Van Soest, Robertson, & Lewis, 1991; Machado et al., 2014; Nunes et al., 2021; Morais, 2021).

Initially, the pulp was heated to 70°C immersed in a neutral detergent solution. In sequence, it was separated by filtration to remove the cell wall. Thus, the cellular compound was separated from the wall (Van Soest, 1991; Morais, 2021).

The acid detergent was then used to dissolve the cellulose, and then remove by filtration, the other compounds of the fraction, through filtration (Morais, 2021).

2.3.4 Characterization of compound bonds

The relationship between the bonds of the constituent compounds of the samples was made by using Fourier Transform Infrared Spectroscopy (FTIR) (Ribeiro, 2016). The analysis consisted of 16 scans, in bands from 400 to 4000 cm^{-1} (Morais, 2021; Nunes et al., 2021), using a model spectrometer Vertex 70 from BRUKER. Sample preparation was carried out by dispersing the sample directly into the equipment's reading laser.

2.3.5 Thermal characterizations

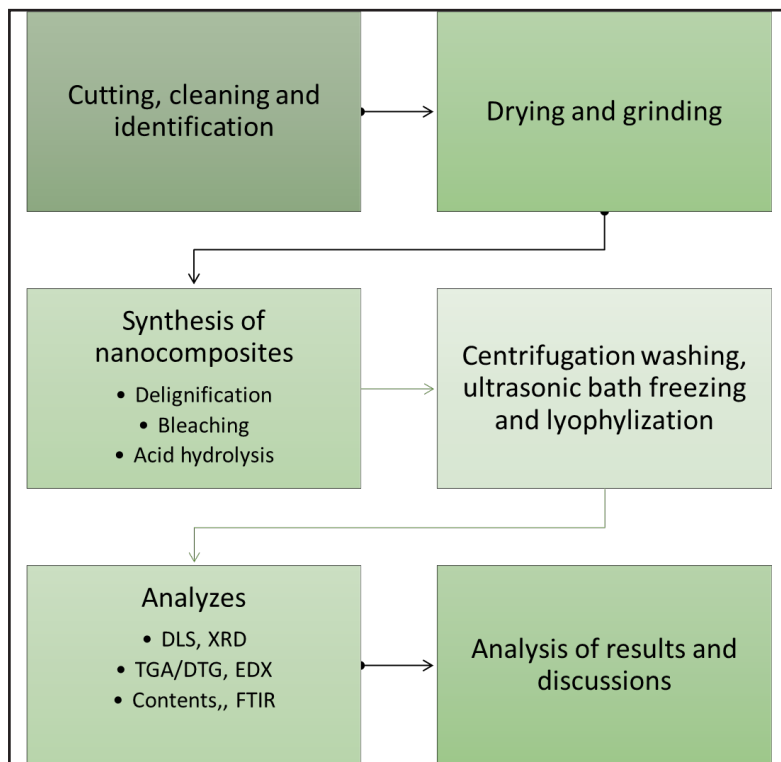
To analyze the behavior of the pulp under conditions of temperature variation, thermogravimetric analysis (TGA) and differential thermal analysis of the sample (DTA) were performed (Cordeiro et al., 2014; Ribeiro, 2016; Júnior, 2012). A calorimeter was used, with a rate of 10 $^{\circ}\text{C}/\text{min}$ until a temperature of 600 $^{\circ}\text{C}$ (Morais, 2021; Nunes et al., 2021). In the DTA, the sample was used in a nitrogen atmosphere, at a rate of 100 mL/min (Nunes et al., 2021).

2.3.6 Characterization of constituent elements and compounds

In order to determine the characteristics of the elements and compounds that constitute the samples, energy-dispersive X-ray spectroscopy (EDX) analysis was performed using a vacuum atmosphere, on the EDX-720 equipment, from the brand SHIMADZU, with two-channel reading, the Ti-U channel with analysis at 50 kV and the Na-Sc channel with analysis at 15 kV, in a vacuum atmosphere and using a 10 mm collimator (Rodrigues; Sousa; Olivier, 2022). Sample preparation was tablet-type: the sample, in powder form, was pressed with the aid of a mechanical press and a force of 5 tons for 1 minute.

The summary of the steps performed is related to the flowchart shown in Figure 5.

Figure 5 – Summary of steps performed during the study



Source: Authors' private collection (July, 2023)

Legend: Steps performed throughout the study: comprising initial steps, from cutting to grinding; sample preparation steps, from delignification to lyophilization; stages of analysis and finalization with results and discussions

3 RESULTS AND DISCUSSIONS

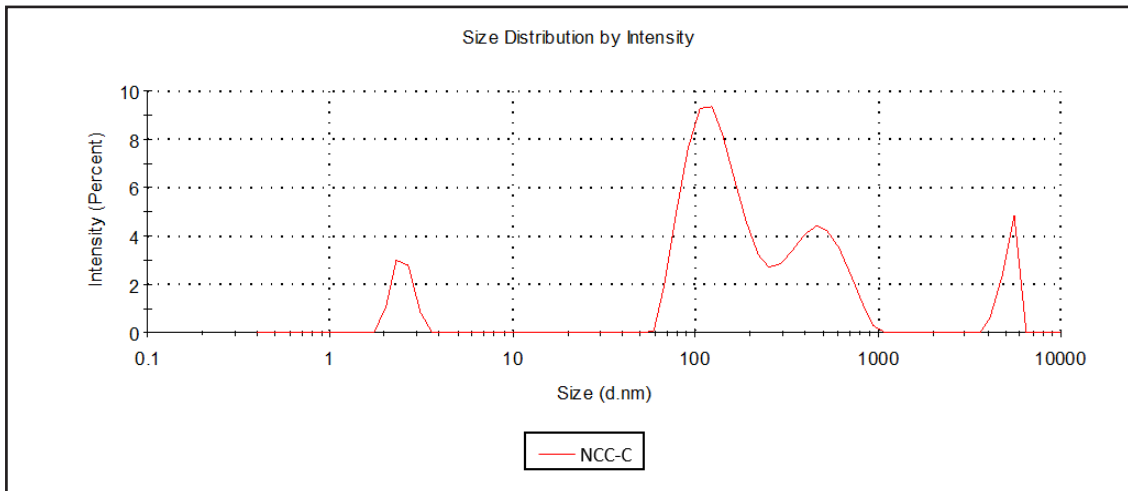
3.1 Results

3.1.1 Distribution of particle diameters

In Figures 6 and 7, the Zetasizer analysis for the NCC-C sample, regarding the size distribution by intensity, demonstrated four size distribution peaks. At 3% of the sample, particles with a diameter of 2.50 nm were verified; at 9%, particles 110 nm in diameter were verified; at 4.20%, particles with 450 nm were verified; at 5%, particles with 5000 nm were verified. The latter, due to its amplitude, is neglected. The

analysis regarding the distribution by volume showed a uniform behavior for the peak distribution, which was only one. At this peak, 30% of the sample indicated a diameter of 1.50 nm.

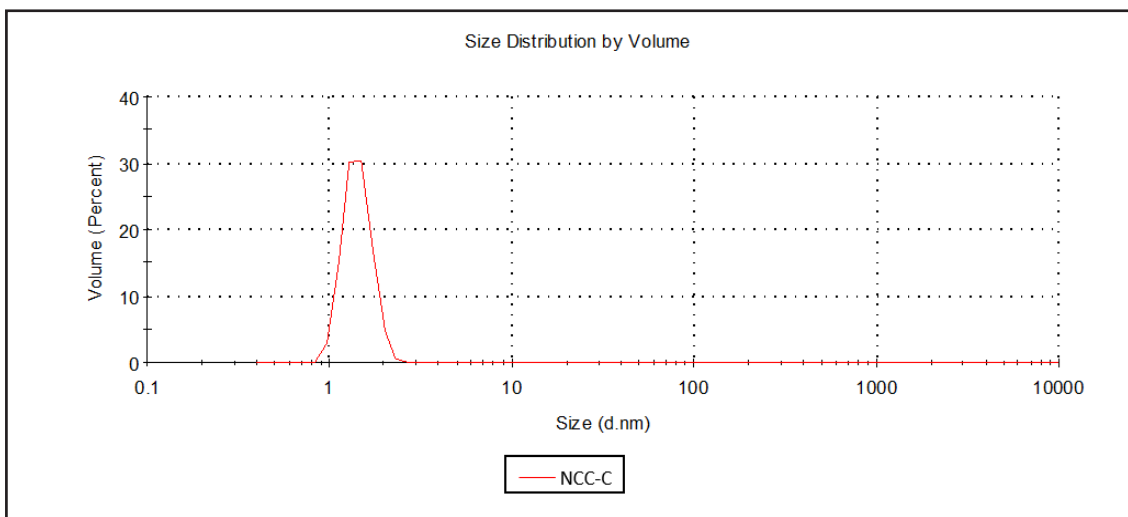
Figure 6 – Distribution of particle sizes by sample NCC-C intensity



Source: Authors' private collection (January, 2023)

Legend: Particle size distribution by intensities of the NCC-C sample, with visualization of bands ranging up to 10000 nm

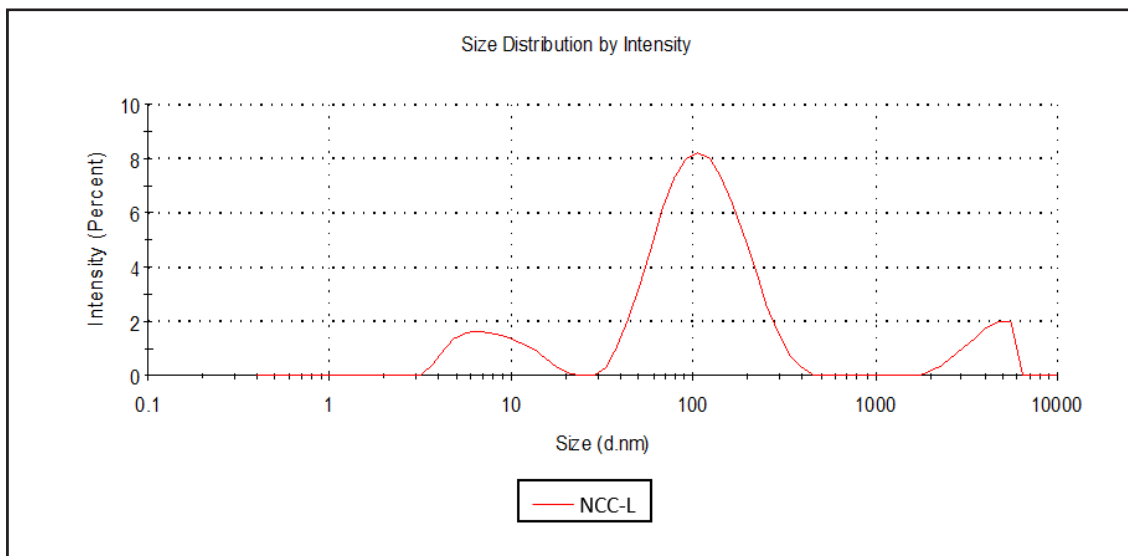
Figure 7 – Distribution of particle sizes by volume of the NCC-C sample



Source: Authors' private collection (January, 2023)

Legend: Particle size distribution by volume of the NCC-C sample, with visualization of bands ranging up to 10000 nm

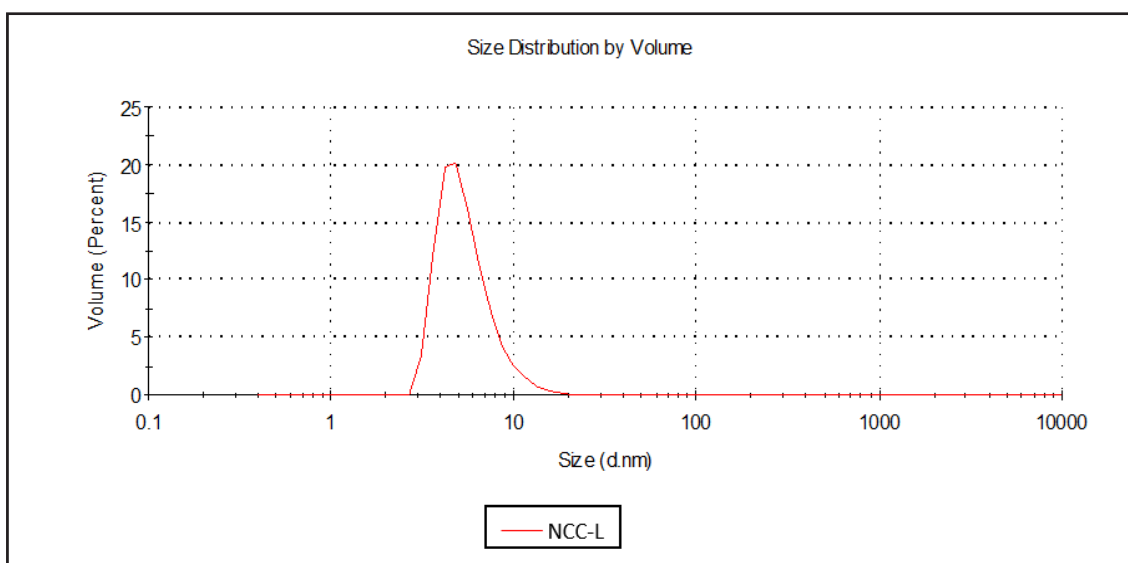
Figure 8 – Distribution of particle sizes by sample NCC-L intensity



Source: Authors' private collection (January, 2023)

Legenda: Particle size distribution by NCC-L sample intensity, with visualization of bands ranging up to 10000 nm

Figure 9 – Distribution of particle sizes by volume of the NCC-L sample



Source: Authors' private collection (January, 2023)

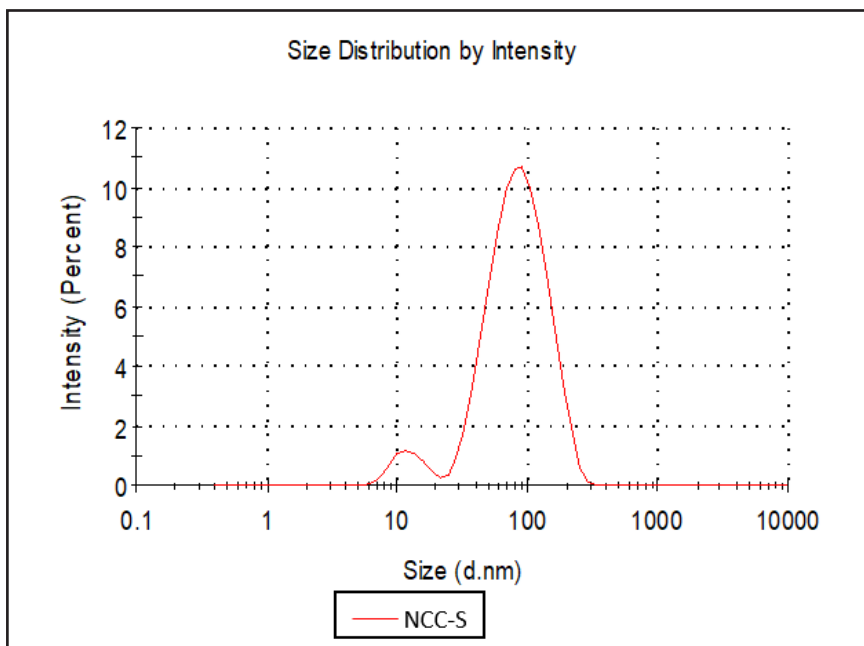
Legend: Particle size distribution by volume of the NCC-L sample, with visualization of bands ranging up to 10000 nm

In Figures 8 and 9, the Zetasizer analysis for the NCC-L sample, regarding the distribution by intensity, showed three distribution peaks. At 1.50% of the sample, particles with a diameter of 6 nm were verified; at 8%, particles 110 nm in diameter

were verified; at 2%, particles with 5500.00 nm were verified. The latter, due to its amplitude, is neglected. The analysis regarding the distribution by volume showed a uniform behavior for the peak distribution, which was only one. At this peak, 20% of the sample indicated a diameter of 4.75 nm.

In Figures 10 and 11, the Zetasizer analysis for the NCC-S sample, in the hydrodynamic diameter distribution by intensity, showed two distribution peaks. At 1% of the sample, particles with a diameter of 12 nm were verified; at 10.75%, particles 89 nm in diameter were verified. The analysis regarding the distribution by volume showed a uniform behavior for the distribution of one peak and a more diffuse behavior for another. In this first peak, 18% of the sample indicated a diameter of 9 nm; in the most diffuse peak, 1.25% of the sample indicated a diameter of 42 nm.

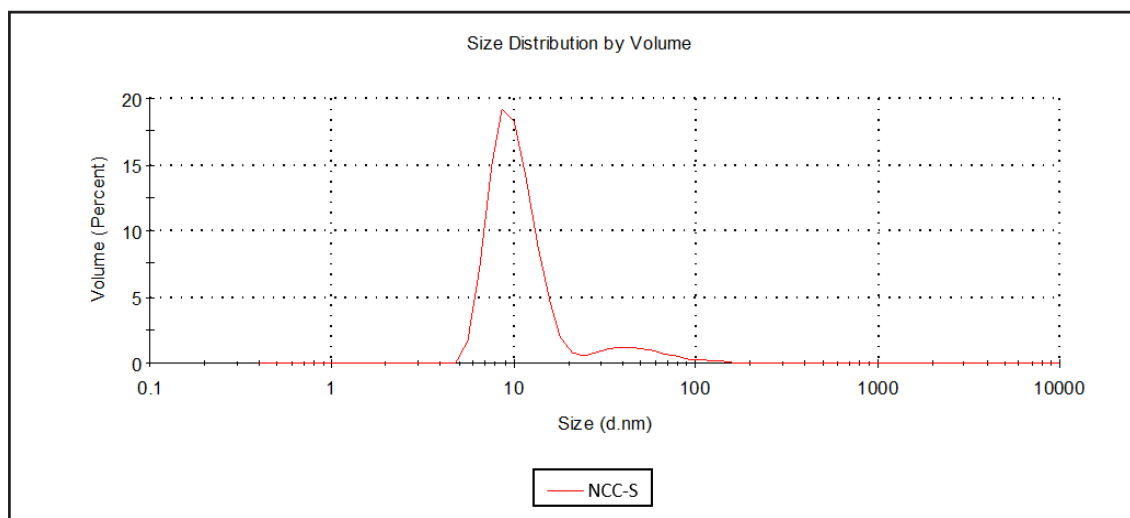
Figure 10 – Distribution of particle sizes by intensity of the NCC-S sample.



Source: Authors' private collection (January, 2023)

Legend: Particle size distribution by intensity of the NCC-S sample, with visualization of bands ranging up to 10000 nm

Figure 11 – Distribution of particle sizes by volume of the NCC-S sample



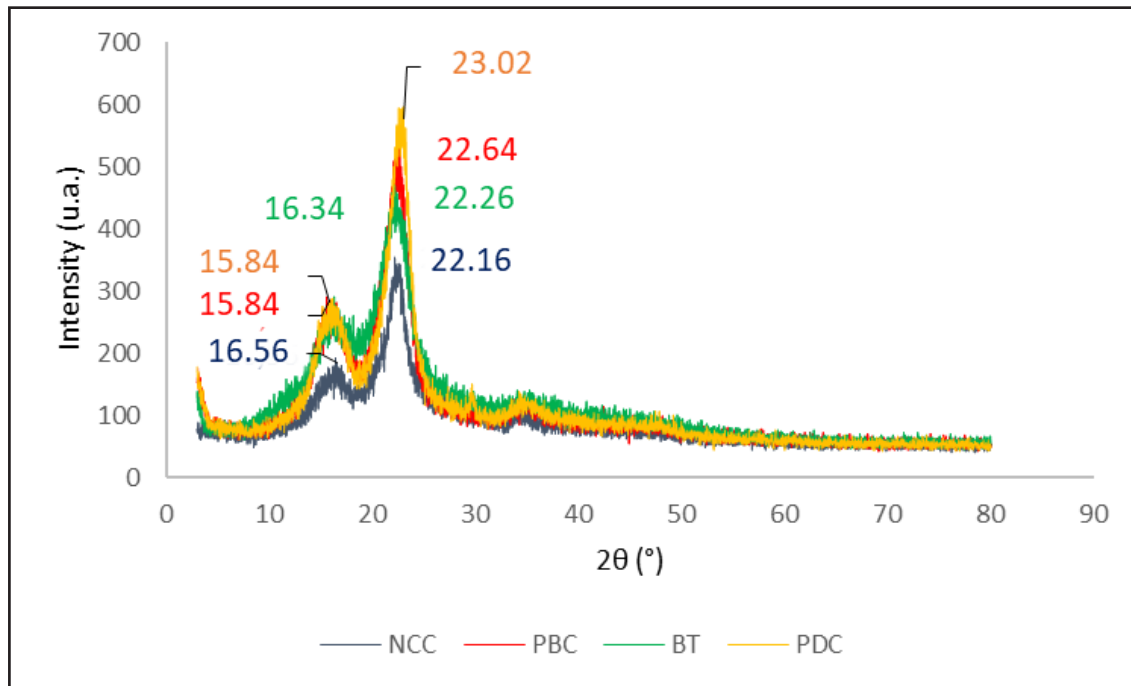
Source: Authors' private collection (January, 2023)

Legend: Particle size distribution by volume of the NCC-S sample, with visualization of bands ranging up to 10000 nm

3.1.2 X-ray diffraction

In Figure 12, the XRD measurements indicate the crystallization characteristics of the samples. In general, the samples demonstrated the behaviors through two peaks, well defined, with high intensity in relation to the other points of the verified samples. The peaks of the BT sample were found at $2\theta=16.34^\circ$ e 22.26° ; the PDC sample showed peaks of $2\theta=15.84^\circ$ e 23.02° ; the PBC sample signaled peaks at $2\theta=15.84^\circ$ e 22.64° and the NCC sample signaled peaks at $2\theta=16.56^\circ$ e 22.16° . It is possible to notice the standardization of the behavior, as the peaks are aligned in nearby regions 2θ , allowing indications of similar characteristics, despite the slightly different variations along their read compositions.

Figure 12 – XRD diffractogram of the samples showing indications of crystallinity



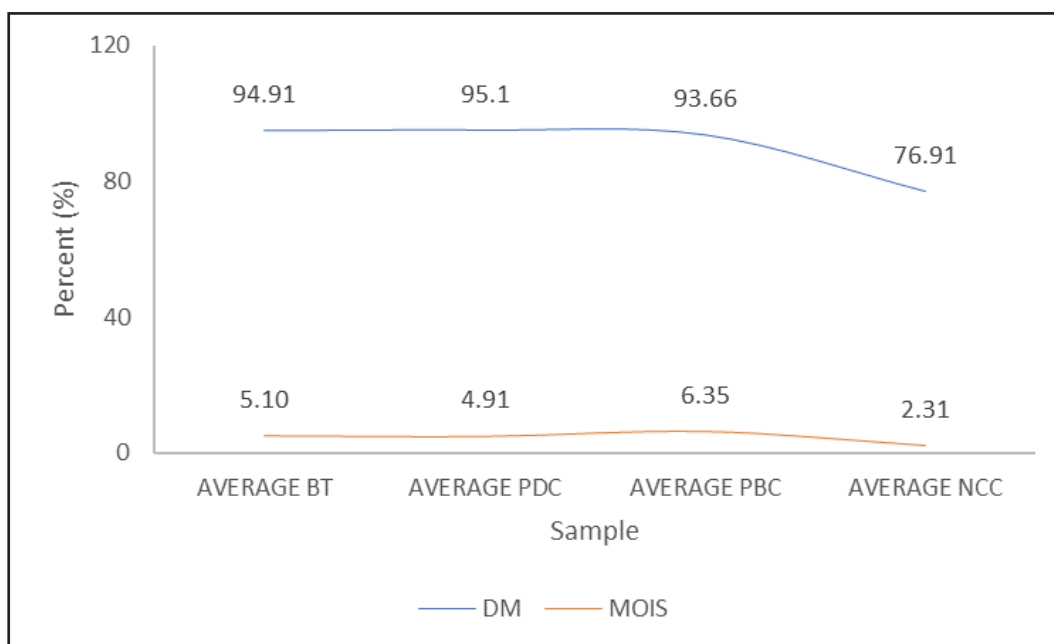
Source: Authors' private collection (August, 2023)

Legend: DRX readings of the sample showing indications of crystallinity for the four types of samples throughout the treatments performed in the synthesis process

3.1.3 Fiber and cellulose content

In Figure 13, the samples portray the steps of the chemical treatment used, with in natura BT sample, sample with initial PDC treatment, sample with intermediate PBC treatment and sample with complete NCC treatment finished. The averages found, relative to three repetitions of the study, show the behavior of the dry matter (DM) and moisture (MOIS) contents of the respective samples. The analysis points to a decrease in the above-mentioned levels, being maximum in the BT sample (with 94.91 and 5.1%, respectively), decreasing to minimum values at the end of the treatment, in the NCC sample (76.91 and 2.31%).

Figure 13 – Dry matter and average moisture contents present in the samples

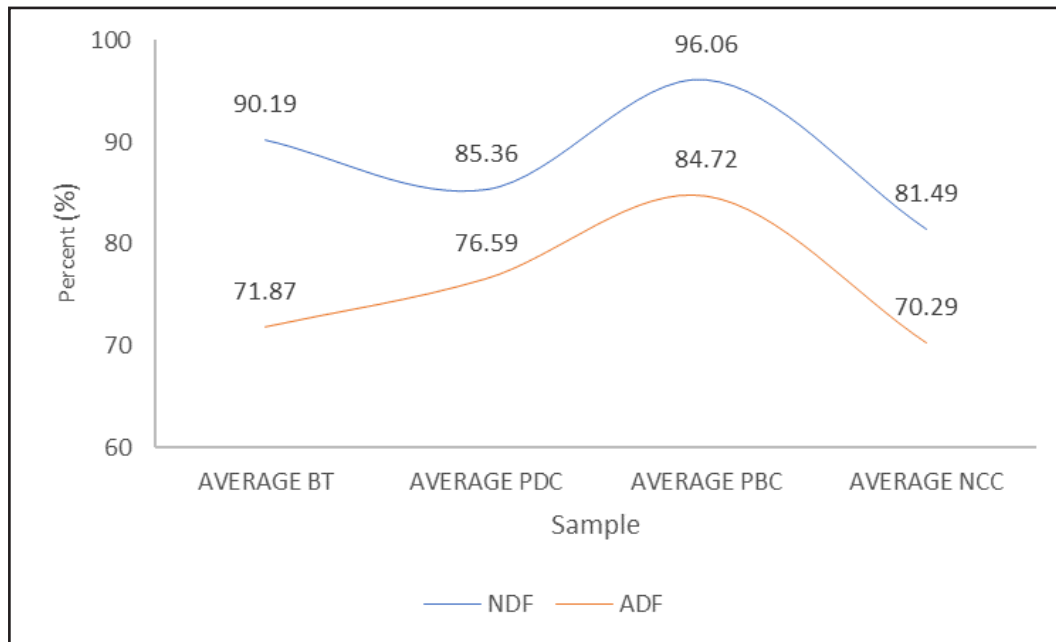


Source: Authors' private collection (February, 2023)

Caption: Average dry matter and moisture contents for the four types of samples throughout the treatments performed in the synthesis process

In Figure 14, the contents of fiber components, namely cellulose, lignin and hemicellulose, are preliminarily verified in this analysis. While cellulose and lignin compounds are related to acid detergent fiber solubility (ADF). Hemicellulose, however, is also related to neutral detergent fiber (NDF) solubility, in addition to ADF. Revealing the nature of these compounds throughout the treatments used in the sample. For the NDF fibers, the indicating behavior reflects peaks in the content, having in the final sample NCC, its lowest value, of 81.49%, in comparison to its highest value, still in the treatment of the PDC sample, with 96.06%. Similarly, with interpretative reservations, ADF fibers have increasing value, from in natura, 71.87%, to the peak exposed in the intermediate treatment of the PDC sample, 84.72%. In the final treatment of the NCC sample, however, the content assumes its lowest percentage, reaching 7.29%. Both NDF and ADF behaviors demonstrate the need for further analyzes on the nature of these found compounds.

Figure 14 – Average contents of NDF and ADF fibers present in the samples

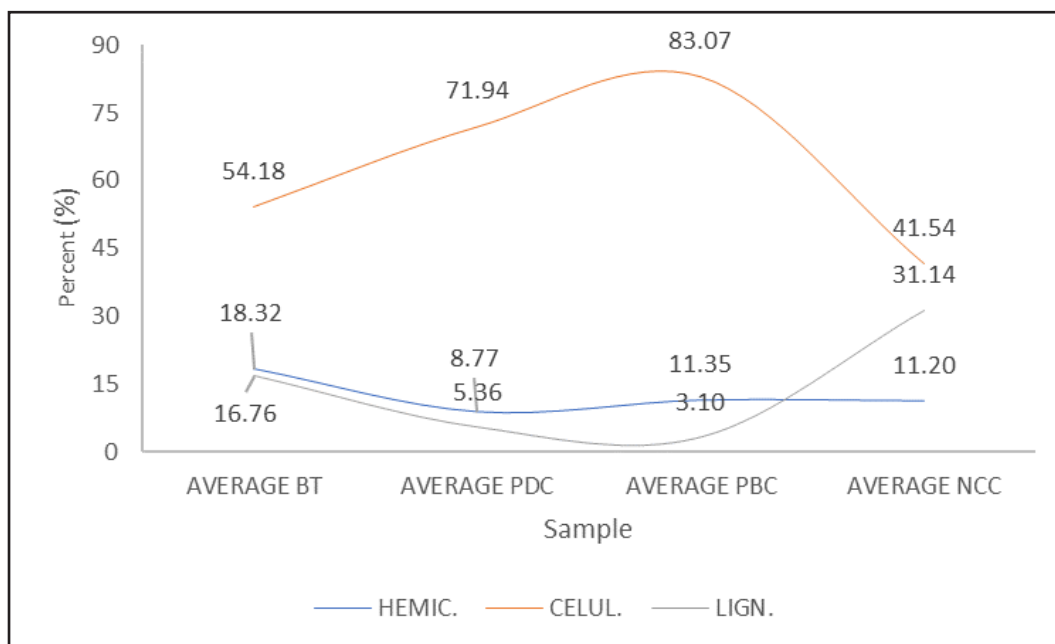


Source: Authors' private collection (February, 2023)

Legend: Average NDF and ADF fiber contents for the four types of samples throughout the treatments performed in the synthesis process

In Figure 15, the cellulose, hemicellulose and lignin contents are indicated. Lignin presents an approximately extreme behavior in the analysis of NDF/ADF fiber content, having an initial peak of 16.76% in the BT sample, being reduced to the lowest value by the PBC treatment, 3.10%, and having a maximum peak in the sample of NCC, with 31.14%. For hemicellulose, the behavior is approximately decreasing, with the maximum value being the initial value of the BT sample, 18.32%, reduced to 11.20% in the NCC sample, which, even though it is not the minimum value expressed by the sample, is among the minimum values. At the end, inversely with the other behaviors, the cellulose content increases to the maximum point of the PBC treatment, 83.07%, being slightly reduced to the minimum value of 41.54%, expressed in the NCC sample. This atypical relationship of levels in relation to the respective treatments urges the need for complementary analyses, this will be exposed later.

Figure 15 – Cellulose, lignin and hemicellulose contents present in the samples



Source: Authors' private collection (February, 2023)

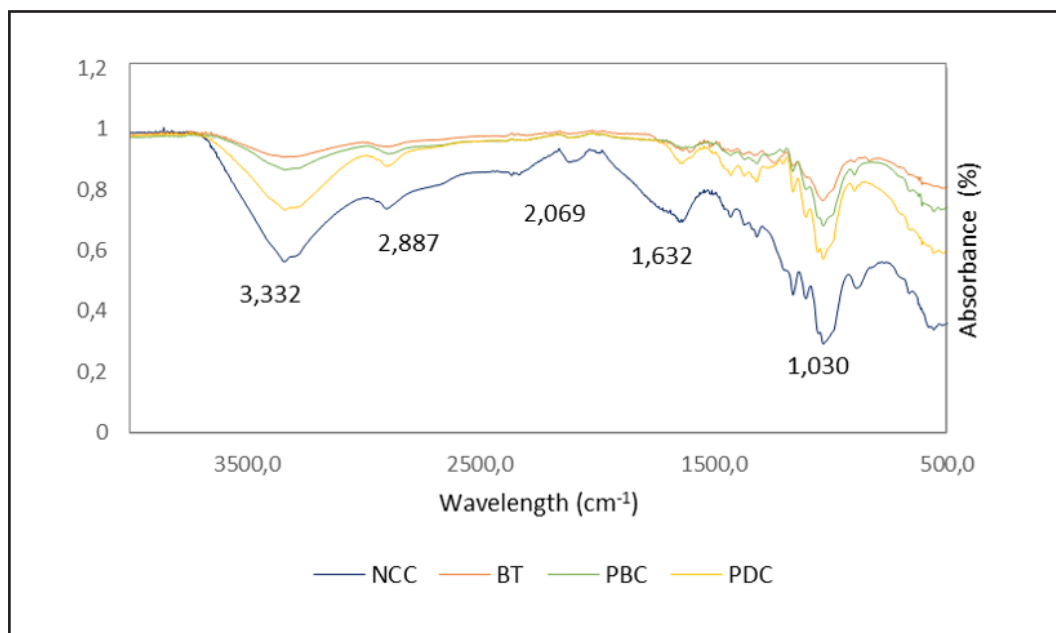
Legend: Average contents of cellulose, lignin and hemicellulose for the four types of samples throughout the treatments performed in the synthesis process

3.1.4 Characterization of compound bonds

In Figure 16, the FTIR spectrum for the four treatments of BT, PDC, PBC and NCC samples are shown. Visibly, it is verified that the material of the samples, for corresponding to the same in different stages, demonstrated the same behavior in terms of peaks, with alteration of decrease in the absorbances corresponding to each sample. Being maximum in the in natura BT sample, and minimum when indicated in the NCC sample, with final treatment. Regarding the peaks, they are common to the four samples, so that this factor becomes interesting in their analysis, as it demonstrates that the compounds present there remain inert throughout the treatment stages, but still significant to the performance of the studied samples. The peaks, common and more expressive throughout the treatment of the samples, are expressed in the regions of wavelengths equivalent to $3,332\text{ cm}^{-1}$ (A), $2,887\text{ cm}^{-1}$ (B), $1,632\text{ cm}^{-1}$ (C) e $1,030\text{ cm}^{-1}$ (D).

Corresponding to other studies, it is possible to verify and interpret the incidence of each peak. In A peak, its occurrence implies the presence of groups of the types OH, CH₃, CH₂ and CH, arising from the processes that degrade the hemicellulose in the sample (Júnior et al., 2019). In B peak, there is a change in the crystallinity of the cellulose, corresponding to the presence of (C-H) and (O-H) bonds (Júnior et al., 2019). The C peak indicates the vibration of the C=O group, resulting from the intrinsic compounds of lignin and cellulose remaining in the samples (Júnior et al., 2019). D Peak, the decrease indicates that cellulose and lignin compounds begin the decomposition process, emphasizing the existence of carbonaceous residues resulting from the previously indicated bonds (Júnior et al., 2019). These results are related to those seen in the analyzes of cellulose, lignin and hemicellulose content, previously seen.

Figure 16 - FTIR spectrum for samples in the spectrum from 400 to 4000 cm⁻¹



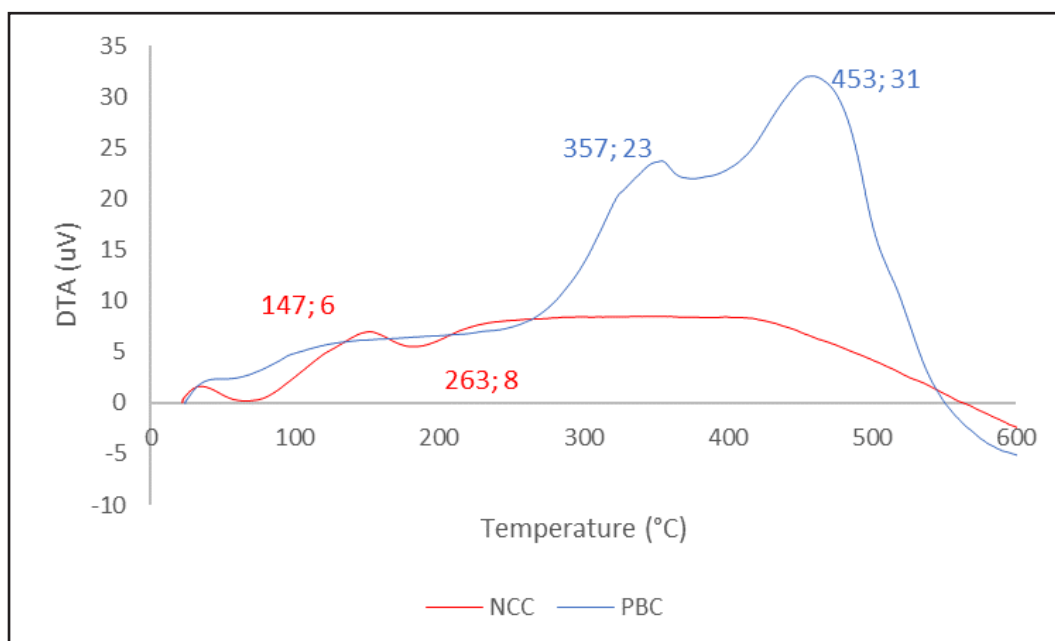
Source: Authors' private collection (May, 2023)

Legenda: FTIR reading for the four types of samples along the treatments performed in the synthesis process, in scans that ranges up to 4000 cm⁻¹

3.1.5 Thermal characterizations

In Figure 17, the behavior of the NCC and PBC samples are shown in relation to the differential thermal variation. In the PBC sample, it is possible to observe that at temperatures up to 300 °C, mass loss occurs in the sample, while at 357 °C and 453 °C, exothermic events occur due to phase change in the amorphous characteristics of the sample. From the last peak, the sample decomposition process begins until the final temperature of 600 °C. For the NCC sample, the initial alteration of the baseline due to degradation of the sample mass occurs approximately up to 147 °C, with stability from 263 °C, without considerable variations from the baseline, indicating inertia to the exothermic and endothermic events up to about 400 °C, where the sample decomposition process begins, up to a final temperature of 600 °C.

Figure 17 – Differential thermal variation analysis of the samples



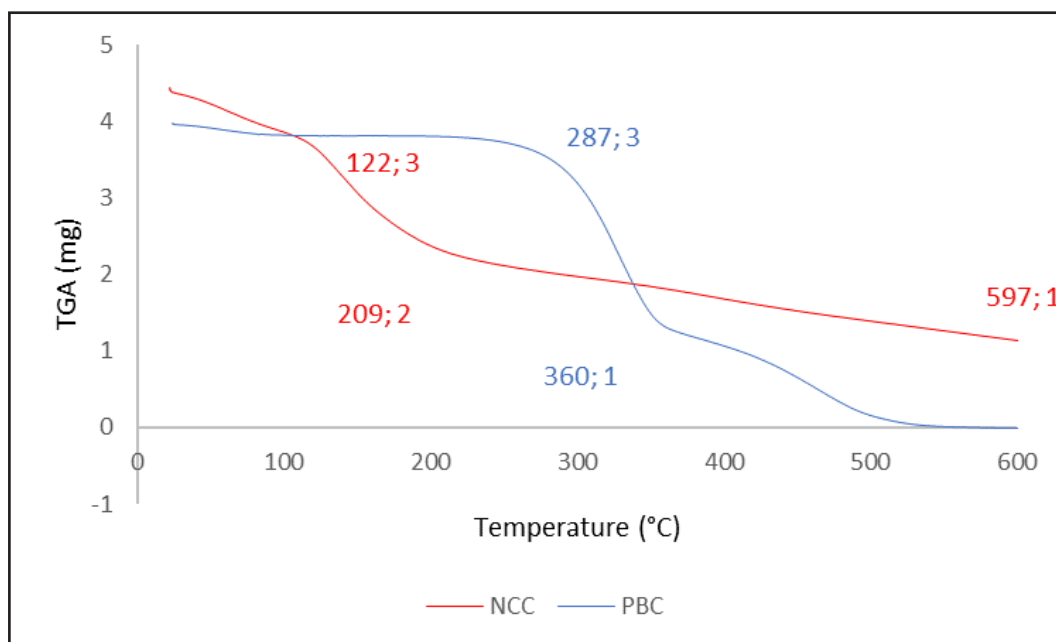
Source: Authors' private collection (May, 2023)

Legend: Differential thermal variation for the two types of samples throughout the final treatments performed in the synthesis process, in the thermal variation up to 600,00 °C

In Figure 18, the behavior of the NCC and PBC samples are shown in relation to the thermogravimetric variation. In the PBC sample, it is possible to observe that at

temperatures up to 287 °C, there is no considerable mass loss in the sample, whereas between this peak and 360 °C, the sample suffers a reduction from 3 to 1 mg, being a value corresponding to 38.30% of the remaining mass of the sample in the last peak. From the last peak, the process of decomposition of the final sample of the sample starts up to about 500 °C, from where, beyond that point, residual materials from the degradation are found. For the NCC sample, the initial mass change of the sample occurs approximately up to 122 °C, with instability indicative of exothermic processes that result in considerable mass loss up to 209 °C, where only 2 mg are found of its previous mass. From this point on, until the final temperature of 600 °C, the sample decomposes in a preserved way, without the formation of residual material.

Figure 18 – Thermogravimetric variation analysis of the samples



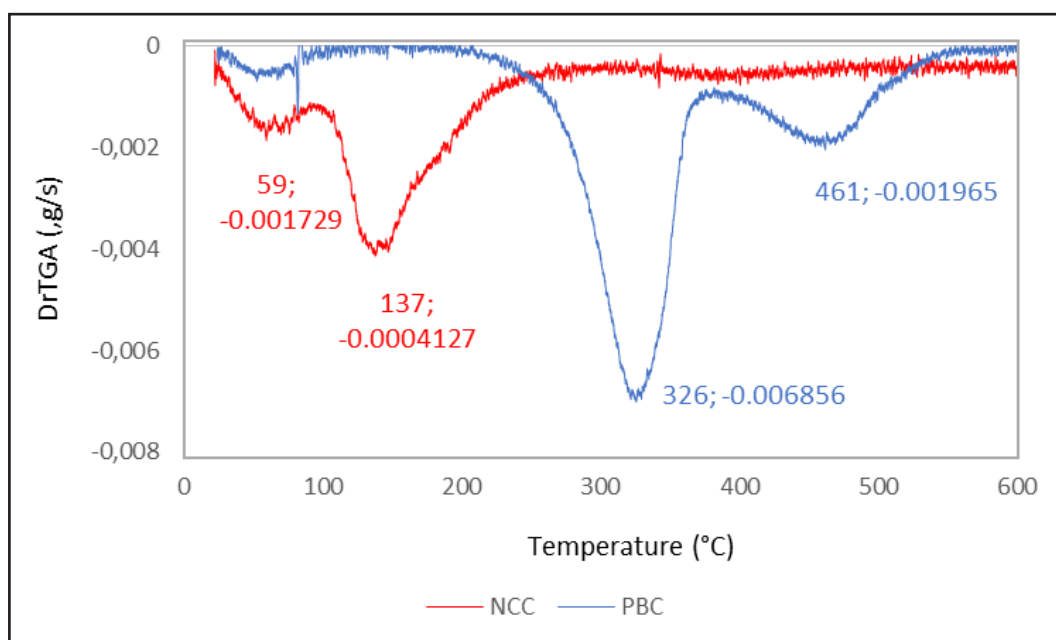
Source: Authors' private collection (May, 2023)

Legend: Thermogravimetric variation for the two types of samples throughout the final treatments performed in the synthesis process, in the thermal variation up to 600,00 °C

In Figure 19, the behavior of the NCC and PBC samples is shown in relation to the interpolated variations between differential thermal and thermogravimetric analysis. In the PBC sample, the peak at 326 °C indicates the great thermal activity with a significant reduction in the mass resulting from exothermic processes, which reduce

along the temperature up to 461 °C, where again the thermal activity reduces until the process thermal differential be completed at 600 °C. In the NCC sample, the behavior demonstrates a lower amplitude than the PBC sample, indicating greater energy stability in the particles. The initial peak, oscillating at 59 °C, with a maximum of 137 °C, shows the mass reduction, in relation to the data in the PBC sample, is in reduction until the end of the thermal variation at 600 °C , again, a significant indication of the thermal stability strongly linked to the compounds of this sample, later characterized.

Figure 19 – Interpolation analysis between differential thermal and thermogravimetric variation of NCC and PBC samples



Source: Authors' private collection (May, 2023)

Legend: Interpolation of differential and thermogravimetric thermal variation for both types of samples throughout the final treatments performed in the synthesis process, in the thermal variation up to 600,00 °C

3.1.6 Characterization of constituent elements and compounds

The qualitative analysis pointed, through the peaks, to the incidence of Rhodium (Rh), Vanadium (V), Copper (Cu), Sodium (Na) and Silicon (Si) compounds. Table 1 below brings the results of the quantitative analysis of compounds.

Table 1 - Percentage intensity of compounds found in the analysis for the PBC sample

Sample		PBC
Compound	Intensity (%)	Standard deviation
Na ₂ O	73.539	6.428
V ₂ O ₅	15.078	0.668
SiO ₂	7.625	0.582
CuO	3.758	0.190
CO ₂	0,000	0

Source: Authors' private collection (June, 2023)

Table 1 shows the existing compounds in the PBC sample, as well as their abundance intensities and correlated standard deviations. In higher proportion, there is the presence of sodium oxide, followed by the presence of vanadium pentoxide. To a lesser extent, there are silicon dioxide and copper oxide, which together add up to just over 10.30% of the sample composition.

3.2 Discussions

The diameters found are related to the results by other authors in the scientific literature. Cotton nanofibers indicated diameters from 14 to 9 nm, being similar to the diameters found for NCC-C, NCC-S and NCC-L (Teixeira et al., 2010). Bacterial cellulose nanocrystals demonstrated diameters in the same range, with peaks indicating diameters of 96.36 and 388 nm (Costa et al., 2017). Thus, it is visible that the results obtained by the NCC-C, NCC-L and NCC-S samples show peaks equivalent to those obtained in related works, characterizing them as nanomaterials.

As for the crystallization of the samples, the XRD analysis allowed, through the readings, important indications about the properties and crystalline characteristics of the samples. The comparison with microcellulose fiber analysis found similar indicators, bringing light to two interpretations which are gradually related to the regions of the peaks found: the peaks of all samples present near the region of $2\theta=18^\circ$,

indicates the presence of amorphous compounds, in which the low intensity reflects a smaller presence of these compounds; the peaks of all samples present near the region between 22° – 23° , indicate the presence of crystals in the samples, especially in the NCC sample, reinforcing its characterization and its capacity for subsequent interaction (Bilcati; Costa; Paulino, 2022). Similar behavior regarding the presence of the amorphous region and the predominance of the crystalline region is found in syntheses of rice husk ash fibers, in silicate compounds, which observed predominance in their readings, according to the scope of intensity in the 20° – 25° region (Moura; Resende; Souza, 2023). Furthermore, the peaks found can also be observed in a similar way to those obtained during the reading of bacterial spherical nanocellulose samples (14.4° and 22.7°), where the crystalline formations point to convergent regions of the indicated peaks (Cesca et al., 2020).

The inclusion of cellulose fibers, on a nano or micro scale, for cement-based composites, demonstrates the implication of use for mechanical and physical properties, in order to accomplish it, the determination of the contents is essentially linked to the desired perspective (Morais, 2021; Bilcati, Costa, Paulino, 2022; Lima et al., 2022; Machado et al., 2022). The contents found for cellulose, hemicellulose and lignin, consequently reflected by the NFD and ADF contents, were above those obtained for other species, such as potato fiber and sweet potato fiber, pine, eucalyptus and *murumuru* (Lima et al., 2022; Machado et al., 2022). However, species with similar values, such as *Guadua bamboo spp.*, in the form of a nanofiber, and the *murumuru* compound, through cellulose microfiber, showed increased mechanical performances in the properties and behavior of integration between cement and cellulose components, which indicates the perspective of application (Morais, 2021; Bilcati, Costa, & Paulino, 2022; Lima et al., 2022).

For the differential thermal and thermogravimetric analysis, the behaviors demonstrated situations in which it was possible to establish parameters that fit the verified samples regarding their use for the cementitious composite. Pozzolanic clays,

materials with compositions and structures that are different from those analyzed in the present samples, despite the endothermic peaks, were subject to observation in them, similar processes of mass loss and residual conservation (Medeiros & Morais, 2020). Bamboo cellulosic pulp *Guadua spp.* obtained behavior similar to that obtained for the PBC sample, possibly due to the relationship between the analyzed and reference species of the study, with exothermic points and residues from decomposition (Morais, 2021). In a parallel made up of thermal analyzes based on cellulose compounds, bacterial cellulose nanocrystals and cellulose acetate gels, common points indicated that the peaks present in the reference curves and in the one obtained from the study converge while three processes occur along the thermal variation: the loss of initial mass, linked to the loss of water intrinsic to the molecules of the sample; the second process is the depolymerization one, resulting from the breaking of bonds suffered by the degradation of cellulose, the last consequent peak for the last range of analysis, reflects the degradation of the carbonaceous residues of the sample (Senna, Menezes, & Botaro, 2013; Costa et al., 2017).

The FTIR analysis showed the results obtained for cellulose, lignin and hemicellulose content. The C, H and O groups, as well as their different connections found, demonstrate this relation. Other studies with cellulose obtained from wood of the species *Corymbia citriodora* and hydrogels based on cellulose acetate, found variations in the peaks, tending to an average proximity of 100 cm^{-1} , pointing to similar slopes in the indication of the behavior of the compounds in the samples, being of them, with more expressive results in NCC samples (Botaro, Santos, & Oliveira, 2009; Júnior et al., 2019).

The XRD analysis showed richness of sodium oxide, vanadium pentoxide and silicon dioxide compounds in the PBC sample, while in the NCC sample, it was possible to observe the abundance of sodium oxide. The results corroborate other analyzes that indicate the efficiency of this technique for verifying oxides and metals, such as zinc and semimetals, in studies analyzing copper layers. (Nyong et al., 2021). The

concentrations of sodium oxide and the lowest content of silicon dioxide are similar to other substances studied, such as oily residues, which have potential for incorporation into concrete, due to the concentrations of the sodium compound being similar to that of concrete, indicating affinity, and the silicon compound content is sufficient and not so high, to the point of triggering alkali-aggregate reactions, which can compromise the durability and resistance of concrete in the long term. (Lira et al., 2015).

The perspective of cellulose nanocomposites application, involves challenges of its synthesis, while the applications include a range of variations which can vary from structural, to food consummation (Dongre, Suryawashi, 2021; Hasan, Walia, 2021; Ahmad et al., 2022). While using it as a structural component, it permeates the preparation and synthesis, resembling works that perform acid hydrolysis, although with particularities related to the methods, which reflect results similar to those found in the present study (Yu et al., 2012; Abdulkhani et al., 2014; Orrabalis et al., 2019; Thipcai et al., 2023). In turn, the characterization through analyzes such as FTIR and TGA/DTA, reflected the similarities with nanocrystal compounds obtained by other species synthesized in alternative methods to those given here throughout the steps performed (Yu et al., 2012; Abdulkhani et al., 2014; Guo; Wu, Xie, 2017; Orrabalis et al., 2019; Thipcai et al., 2023). Therefore, it is notorious that the execution of the processes established consistency with studies consecrated in the current scientific literature.

4 CONCLUSIONS

The nanofiber and nanocrystal obtained from the cellulose of the native bamboo *Guadua weberbaeuri* were obtained and characterized satisfactorily. The analyzes showed that they are predominantly crystalline nanomaterials, have high levels of cellulose and low levels of lignin and hemicellulose, have compatible bonds with similar carbonaceous compounds, are rich in sodium oxides and have the presence of silica, having chemical affinity with the compounds present. in cement, indicating that it is suitable for incorporation into the cementitious composite. Thermal analysis

indicated high stability and high degradation temperature, proving its use as structural reinforcement in structures with a long service life. The present study showed that there are favorable indications for incorporation in the cementitious composite, corroborating values of sustainability and nanotechnology can be applied in civil construction.

ACKNOWLEDGEMENTS

To CAPES; to Maria Rosália Nascimento; to Ambiental Amazônia, in the person of Emanuel Amaral; to FUNTAC; to Laboratório de Síntese de Materiais Cerâmicos, in the person of professor Ana Cristina and to EMBRAPA.

REFERENCES

- Abdulkhani, A., Hosseinzadeh, J., Ashori, A., Dadashi, S., & Takzare, Z. (2014). Preparation and characterization of modified cellulose nanofibers reinforced polylactic acid nanocomposite. *Polymer Testing*, 35, 73–79.
- Ahmad, M. I., Farooq, S., & Zhang, H. (2022). Recent advances in the fabrication, health benefits, and food applications of bamboo cellulose. *Food Hydrocolloids for Health*, 2, 100103.
- Alvarenga, B. L., Junior, L. M., Faria, D. L., Dias, M. C., Alvarenga, V. L., Mendes, L. M., & Junior, J. B. G. (2022). Physical and mechanical evaluation of gypsum composites reinforced with *Bambusa tuldoidea* fiber. *Matéria (Rio de Janeiro)*, 27(2), p. e13187.
- Auersvaldt, B. L., Lay, L. A., & Miranda, T. L. (2019) Incorporation of bamboo plant fibers into concrete to replace synthetic fibers. In: *Anais IX Congresso Brasileiro de Engenharia de Produção*.
- Barbosa, A. M., Rebelo, V. S. M., Martorano, L. G., & Giacon, V. M. (2019) Characterization of açai particles aiming at their potential use in civil construction. *Matéria (Rio de Janeiro)*, v. 24, n. 3, p. e12435, 2019.
- Bilcati, G. K., Costa, M. R. M. M., & Paulino, R. S. (2022). Effect of multi-scale crystalline cellulose-microcellulose fiber reinforcement on the hydration phase of Portland cement pastes. *Matéria (Rio de Janeiro)*, 27(4), e20220220.
- Botaro, V. R., Santos, C. G., & Oliveira, V. A. (2009). Superabsorbent hydrogels based on cellulose acetate modified by dianhydride 3,3', 4,4' tetracarboxylic benzophenone (BTDA): synthesis, characterization and physicochemical studies of absorption. *Polímeros*, 19(4), 278–284.

- Brito, F. M. S., Paes, J. B., Oliveira, J. T. S., Arantes, M. D. C., & Neto, H. F. (2015). Anatomical and physical characterization of giant bamboo (*Dendrocalamus giganteus* Munro). *Floresta e Ambiente*, 22(4), 559-566.
- Campos, C. I., Silva, A. P. S., Aquino, V. B. M., Christoforo, A. L., & Lahr, F. A. (2023). RAnalysis of the effect of incorporating ZnO nanoparticles on the physical and mechanical properties of MDF panels. *Ambiente Construído*, 23(1), 171–182, jan.
- Cesca, K., Netto, M. S., Ely, V. L., Dotto, G. L., Foletto, E. L., & Hotza, D. (2020). Synthesis of spherical bacterial nanocellulose as a potential silver adsorption agent for antimicrobial purposes. *Cellulose Chem. Technol.*, 54 (3-4), 285-290.
- Correia, V. C. (2011). *Production and characterization of organosolve bamboo pulp for reinforcement of cementitious matrices*. Dissertação (Zootecnia). Universidade de São Paulo, Pirassuninga - SP.
- Costa, J. F., Garcia, M. C. F., Apati, G. P., Barud, H. S., Schneider, A. L. S., & Pezzin, A. P. T. (2017). Bacterial cellulose nanocrystals: from obtaining, under different hydrolysis conditions, to incorporation as reinforcement in poly(L-lactic acid). *Matéria (Rio de Janeiro)*, 22.
- Dias Júnior, A. F., Oliveira, R. N., Deglise, X., Souza, N. D., & Brito, J. O. (2019). Infrared spectroscopy analysis on charcoal generated by the pyrolysis of *Corymbia citriodora* wood. *Matéria (Rio de Janeiro)*, v. 24, n. 3, p. e12387.
- Dongre, M., & Suryawashi, V. B. (2021). Analysis of cellulose based nanocomposites & potential applications. *Materials Today: Proceedings* 45, 3476–3482.
- Goetz, N. M., Kunst, S. R., Morisso, F. D. P., Oliveira, C. T., & Machado, T. C. (2022). Study of the efficiency of using bamboo as a biosorbent in the removal of methylene blue. *Matéria (Rio de Janeiro)*, 27(3), e20220065.
- Guo, X., Wu, Y., & Xie, X. (2017). Water vapor sorption properties of cellulose nanocrystals and nanofibers using dynamic vapor sorption apparatus. *Scientific Reports*, 7, 14207, DOI:10.1038/s41598-017-14664-7.
- Hasan, I., & Walia, S. (2021). A review on properties and challenges associated with cellulose nanocrystals and nanocomposites. *Materials Today: Proceedings* 45, 3365–3369.
- Jesus, L. C. C., Luz, S. M., Leão, R. M., Zattera, A. J., & Amico, S. C. (2019). Thermal behavior of recycled polystyrene composites reinforced with sugarcane bagasse cellulose. *Matéria (Rio de Janeiro)*, v. 24, n. 3, p. e12421.
- Lima, W. A. S., Souza, A. C. A., Brabo, D. R., Junior, J. L. L., & Dias, C. G. B. T. (2022). Development and characterization of a polymeric composite from murumuru endocarp (*Astrocaryum murumuru* Mart.) and recycled polyolefins. *Matéria (Rio de Janeiro)*, 27(4), e20220160.
- Lira, Y. C., Mendonça, A. M. G. D., Alves, M. H. N., Costa, D. B., & Filho, M. B. C. (2015). Analysis of the alkaline equivalent of oily residue from the petroleum E&P industry and Portland cement for use in concrete. In: *Anais I Congresso Nacional de Engenharia de Petróleo, Gás Natural e Biocombustíveis*.

- Machado, B. A. S., Reis, J. H. O., Silva, J. B. S., Cruz, L. S., Nunes, I. L., Pereira, F. V., & Druzian, J. I. (2014). Obtaining nanocellulose from green coconut fiber and incorporating it into biodegradable starch films plasticized with glycerol. *Quim. Nova*, 37(8), 1275-1282.
- Machado, M. C., Corrêa, M. N., Kozloski, G. V., Oliveira, L., Brauner, C. C., Barbosa, A. A., Cardoso, K. B., & Pino, F. A. B. (2022). Sweet potato (*Ipomea batatas*) feed affects intake, digestibility and nitrogen retention of ovine fed with ryegrass hay (*Lolium multiflorum* Lam. *Arq. Bras. Med. Vet. Zootec.*, 74(1), 169-175.
- Medeiros, J. L. G., & Morais, C. R. S. (2020). Application of thermoanalytical techniques (TGA/DTA) to evaluate the thermal behavior of clay samples to obtain pozzolans. *Divulgação científica e tecnológica do IFPB*. 50.
- Mendes, A. R., Vanderlei, R. D., & Basso, M. A. (2023). Analysis of the crystalline nanocellulose dispersion process for the production of cementitious composites. *Ambiente Construído*, 23(1), 183-196.
- Miranda, E. H.N., Silva, G.A., Gomes, D.A.C., Silveira, M. N. L., Vitorino, F. C., & Ferreira, S. F. (2022). Effect of different wood and bamboo species on the hydration of Portland cement-based matrices. *Matéria (Rio de Janeiro)*, 27(4), e20220194.
- Morais, C. D. N. (2021). *Production and use of cellulose nanofibers from taboca (Guadua spp) to reinforce cementitious composites*. Dissertação (Ciência, Inovação e Tecnologia). Universidade Federal do Acre, Rio Branco – AC.
- Moura, C. A. M., Resende, J. A. L. C., Souza, K. C. (2023). Characterization of Portland cement pastes with addition of silica aiming the immobilization of Cr(VI). *Ambiente Construído*, 23(3), 245-261.
- Nunes, M. R. S., Ramos, D. P., Morais, C. D. N., Sena, A. E. C., Ramos, A. L. R., Rodriguez, F. R., & Faria, F. S. E. D. V. (2021). Preparation and characterization of Guadua weberbaueri bamboo pulp: technology. *SAJEBTT*, Rio Branco, UFAC, 8(2), 217-232.
- Nyong, A. E., Udoh, G., Joachim, J. A. A., Nsi, E. W., & Rohatgi, P. K. (2022). Study of the morphological Changes and the Growth Kinetics of the Oxides Formed by the High Temperature Oxidation of Cu-32.02% Zn-2.30% Pb Brass. *Materials Research*. DOI: <https://doi.org/10.1590/1980-5373-MR-2021-0173>. 25:e20210173.
- Orrabalís, C., Pampilo, L. G., Calderón-Londoño, C., Trinidad, M., & García, R. M. (2019). Characterization of Nanocellulose Obtained from *Cereus Forbesii* (a South American cactus). *Materials Research*, 22(6), e20190243.
- Pego, M. F. F., Bianchi, M. L., & Veiga, T. R. L. A. (2019). Evaluation of the properties of sugarcane and bamboo bagasse for pulp and paper production. *Rev. Cienc. Agrar.*, 62.
- Pereira, A. L. S., Cordeiro, E. M. S., Nascimento, D. M., Morais, J. P. S., Sousa, M. S. M., & Rosa, M. F. (2014). Extraction and characterization of nanocellulose from banana pseudostem fibers. In: *Anais V Congresso Norte-Nordeste de Pesquisa e Inovação*.

- Pereira, M. A. R. (2012). *Bamboo project: introduction of species, management, characterization and applications*. Tese (Design e Construção com Bambu). Universidade Estadual Paulista Julio de Mesquita Filho, Bauru - SP.
- Pescarolo, A., Silva, S. H. L., Pinto, M. C. C., & Costa, M. R. M. M. (2022). The influence of cellulose microfibrils on fresh state of mortars. *Ambiente Construído*, 22(1), 179–190.
- Rambo, M. K. D., Rambo, M. C. D., Almeida, K. J. C. R., & Alexandre, G. P. (2015) Study of Thermogravimetric Analysis of Different Lignocellulosic Biomasses Using Principal Component Analysis. *Ciência e Natura*, [S.l.], 37(3), 862–868. DOI: 10.5902/2179460X18332. Retrieved from: <https://periodicos.ufsm.br/cienciaenatura/article/view/18332>.
- Ribeiro, F. W. M. (2016). *Production of biocomposites from polybenzoxazine matrix derived from LCC reinforced with bamboo fibers*. Dissertação (Química Orgânica). Universidade Federal do Ceará, Fortaleza - CE.
- Rodrigues, S. D. S., Sousa, J. G. G., & Olivier, N. C. (2022). Effects of accelerated aging on beta gypsum with the addition of water-repellent putty. *Ambiente Construído*, 22(4), 355–369.
- Rosa, M.F., Medeiros, E.S., Malmonge, J.A., Gregorski, K.S., Wood, D.F., Mattoso, L.H.C., Glenn, G., Ortsb, W.J., & Imam, S.H. (2010). Cellulose nanowhiskers from coconut husk fibers: Effect of preparation conditions on their thermal and morphological behavior. *Carbohydrate Polymers*, 81, 831-92.
- Samir, M. A. S. A., Alloin, F., & Dufresne, A. (2005). Review of recent research into cellulosic whiskers, their properties and their application in nanocomposite field. *Biomacromolecules* 6, 612-626.
- Sasamori, A. M., Pires, P. G. P., Lemos, A. L., & Santana, R. M. C. (2022). Influence of lignin type on the characterization of natural fiber polymer composites. *Ciência e Natura*, [S. l.], 44, e14. DOI: 10.5902/2179460X68827.
- Senna, A. M., Menezes, A. J. & Botaro, V. R. (2013). Study of crosslink density in superabsorbent gels obtained from cellulose acetate. *Polímeros*, 23(1), 59–64.
- Silvestro, L., Ruviaro, A. S., Lima, G. T. S., Matos, P. R., Rodriguez, E., & Gleize, P. J. P. (2023). Sonicating polycarboxylate-based superplasticizer for application in cementitious matrix. *Revista IBRACON de Estruturas e Materiais*, 16(2), e16205.
- Teixeira, E. M., Oliveira, C. R., Mattoso, L. H. C., Corrêa, A. C., & Paladin, P. D. (2010). Cotton nanofibers obtained under different conditions of acid hydrolysis. *Polímeros*, 20(4), 264–268.
- Thipchai, P., Punyodom, W., Jantanasakulwong, K., Thanakkasaranee, S., Hinmo, S., Pratinthong, K., Kasi, G., & Rachtanapun, P. (2023). Preparation and Characterization of Cellulose Nanocrystals from Bamboos and Their Application in Cassava Starch-Based Film. *Polymers* 15, 2622. <https://doi.org/10.3390/polym15122622>.

Van Soest, P. J., Robertson, J. B., & Lewis, B. A. (1991). Methods for dietary fiber, neutral detergent fiber, and nonstarch polysacchrides in relation to animal nutrition. *Journal Dairy Scientific*, 74, p.3583-3597.

Yu, M., Yang, R., Huang, L., Cao, X., Yang, F., & Liu, D. (2012). PREPARATION AND CHARACTERIZATION OF BAMBOO NANOCRYSTALLINE CELLULOSE. *BioResources* 7(2), 1802-1812.

Authorship contributions

1 – Tiago Henrique da Costa Viana

Graduated in Civil Engineering from the Federal University of Acre. Specialist in Budgeting, Planning and Control for Civil Construction and Occupational Safety Engineering. Postgraduate in Science, Innovation and Technology for the Amazon from the Federal University of Acre.

<https://orcid.org/0000-0002-1354-2031> • tiagohcviana@gmail.com

Contribution: conceptualization, methodology, validation, data curation, formal analysis, investigation, writing – first formal writing, writing – review and editing, data visualization (infographics, flowcharts, tables, graphs), supervision, project administration

2 – Antonia Eliane Costa Sena

Pharmacist, graduated in 2021, has a postgraduate degree in Clinical and Hospital Pharmacy, completed a master's degree at the Federal University of Acre in the Science, Innovation and Technology for the Amazon program.

<https://orcid.org/0000-0003-3506-9270> • elianesena89@gmail.com

Contribution: conceptualization, methodology, software, validation, data curation, formal analysis, investigation, resources, data curation

3 – Maurício da Silva Souza

Civil Engineer graduated from the Federal University of Acre, currently studying for a Master's degree in Science, Innovation and Technology for the Amazon in the area of water resources and nanotechnology, studying for a Master's degree in BIM - Tools and Processes at the IPOG postgraduate institute.

<https://orcid.org/0000-0003-4364-0836> • mauriciosouza@gmail.com

Contribution: conceptualization, methodology, software, validation, data curation, formal analysis, investigation, resources, data curation

4 – Bruno Roseno de Souza Maia

Has a degree in Electrical Engineering, a specialization in Automation and is currently studying for a master's degree in the Postgraduate Program in Science, Innovation and Technology for the Amazon.

<https://orcid.org/0009-0006-8839-7007> • brunoroseno.maia@gmail.com

Contribution: conceptualization, methodology, software, validation, data curation, formal analysis, investigation, resources, data curation

5 – Yuri Sotero Bomfim Fraga

Substitute professor at the Department of Civil and Environmental Engineering at UnB in the area of construction systems and construction materials. PhD in Civil Engineering from the Graduate Program in Structures and Civil Construction at UnB

<https://orcid.org/0000-0002-0426-4615> • yuri.fraga@ufac.br

Contribution: conceptualization, methodology, software, validation, data curation, formal analysis

6 – Marcelo Ramon da Silva Nunes

Degree in Chemistry from the Federal University of Alagoas. PhD in Biodiversity and Biotechnology from the Legal Amazon Biodiversity and Biotechnology Network - BIONORTE in partnership with the Federal University of Acre. Currently a full-time lecturer at the Federal Institute of Acre.

<https://orcid.org/0000-0002-5100-7865> • marcelo.nunes@ifac.edu.br

Contribution: conceptualization, methodology, software, validation, data curation, formal analysis

7 – José Roberto de Lima Murad

Associate Professor III of Civil Engineering at the Federal University of Acre. Has experience in Civil Engineering, with an emphasis on Structures and the Environment. PhD in Civil Engineering from the Fluminense Federal University.

<https://orcid.org/0000-0002-1394-5885> • murad@ufac.br

Contribution: writing – review and editing, supervision, project administration

8 – Anselmo Fortunato Ruiz Rodriguez

Bachelor's degree in Physics from the Universidad Nacional Mayor de San Marcos in Lima - Peru. Specialization in Nuclear Energy under a UNI-IPEN agreement. PhD in Physics from the University of Brasília.

<https://orcid.org/0000-0002-3034-183X> • anselmo.rodriguez@ufac.br

Contribution: writing – review and editing, supervision, project administration

How to quote this article

Viana, T. H. da C., Sena, A. E. C., Souza, M. da S., Maia, B. R. de S., Fraga, Y. S. B., Nunes, M. R. da S., Murad, J. R. de L., & Rodriguez, A. F. R. (2024). Synthesis and characterization of nanofibers and nanocrystals of cellulose from *Guadua weberbaueri*. *Ciência e Natura*, Santa Maria, 46, e85624. <https://doi.org/10.5902/2179460X85624>.